Colloid Polym Sci 278:491–501 (2000)

ORIGINAL CONTRIBUTION

F. Jones
H. Cölfen
M. Antonietti

Iron oxyhydroxide colloids stabilized with polysaccharides

Received: 7 September 1999
Accepted in revised form: 6 December 1999

F. Jones · H. Cölfen (✉) · M. Antonietti
Max Planck Institute of Colloids & Interfaces, Colloid Chemistry
14424 Potsdam, Germany
e-mail: helmut.coelfen@mpikg-golm.mpg.de
Tel.: +49-331-5679513
Fax: +49-331-5679502

Abstract Neutralization of iron salts in aqueous solutions of κ-carrageenan and cellulose sulfate results in iron oxyhydroxide–polysaccharide hybrid colloids with unusual pH stability up to pH 13. It is shown that both polysaccharides form a tight polymer layer surrounding the inorganic particles, which in the case of κ-carrageenan is cross-linked by helical domains forming a self-assembled nanoreactor. The stabilized iron oxyhydroxide particles can undergo further reactions, for example, it is possible by a chemical reaction to produce stabilized magnetite particles. Repetition of the loading/neutralization steps in the reaction results in hybrids with iron contents much higher than the stoichiometric balance of iron and functional groups of the polymer (greater than 100% Fe/SO_4^-). This combination of high iron content with a natural polysaccharide stabilizer makes these colloids interesting for a number of applications, for example, for nutritional purposes or as contrasting agents for tomography.

Key words Self-assembled nanoreactor · Nanoparticles · Polysaccharides · Colloid stabilization · Iron oxide

Introduction

The generation of well-defined inorganic nanoparticles and their exploitation in modern materials has been of major interest in recent years [1–5]. This is because nanoparticles offer an exciting range of novel optical, magnetic or electronic properties. Inorganic nanoparticles are also found in relative abundance in natural organisms which have the ability to mineralize the particles under relatively mild conditions and with unique morphologies designed for their particular end use [6–9]. If such processes could be understood and mimicked, production of advanced materials would be relatively safe and simple. Colloidal iron oxides are of particular interest due to their magnetic, mechanical as well as optical properties. In natural systems the magnetic properties of magnetite nanocolloids (Fe_3O_4) are exploited by magnetotactic bacteria for orientation purposes (we recommend to the interested reader Ref. [9], where the alignment of such iron oxide colloids within the living cells is nicely illustrated). Some mollusks, the chitons, use the abrasive properties of embedded magnetite colloids to strengthen their teeth [9].

Literature related to biological iron oxyhydroxide nanoparticle production mainly focuses on the naturally occurring protein assembly ferritin [10–14], while literature on nonbiological systems exists on dextran sulfates and starch hydrolysis products [15–21]. All these studies have shown stability at pH < 11. The present article investigates the effects of two ionic, sulfate-containing polysaccharides, cellulose sulfate (cellulose-SO_4) and κ-carrageenan (a naturally occurring polymer harvested from seaweed), on iron oxyhydroxide precipitation. The structural formula of both polymers is shown in Fig. 1.

Previously, it was found that the amount of stabilized iron could be correlated to the number of charged groups present in the polymer [15], i.e. both sulfate and

carboxylate groups. We chose, therefore, polysaccharides containing only one functional group and whose charge density is known. The cellulose-SO_4 has a similar charge density to the κ-carrageenan for comparison while ι-carrageenan and λ-carrageenan contain two and three sulfate groups per repeat unit (two sugar rings), respectively. Carrageenans are already widely used in food and pharmaceutical products and are nontoxic and water-soluble [22]. κ-carrageenan and ι-carrageenan are known to form strong gels under certain conditions, while λ-carrageenan only forms a weak gel [22–25].

Mineralization of these polymers was compared to that reported in previous literature [15–21] on dextran sulfate and polysaccharides to elucidate the mineral polymer associations. The stability dependence of the iron oxyhydroxide particles on the type and the amount of polymer was investigated by the use of analytical ultracentrifugation (AUC) and dynamic light scattering (DLS). In addition, we explored some of the material properties of the resulting hybrid systems, i.e. absorption behavior for coloristic purposes.

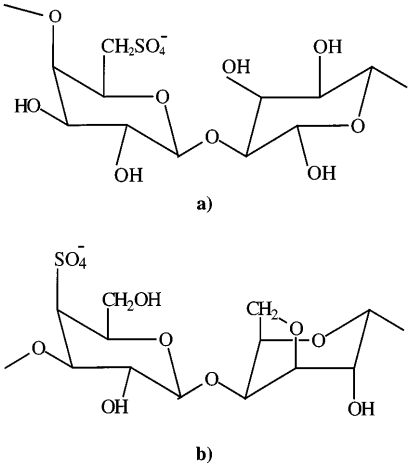

Fig. 1 **a** Repeat unit of the idealized cellulose sulfate (*cellulose-SO_4*) structure with a degree of substitution of 0.5 and **b** schematic diagram of the idealized structure of the repeat unit for κ-carrageenan

Experimental

Methods

The carrageenan solution was prepared by boiling 2 g polymer in 500 ml water and by diluting after cooling to the appropriate concentration. The other polymers were dissolved by stirring overnight. All polymers were prepared at 2 g l^{-1}. Mineralization of the polymer–iron solution was conducted as described in Ref. [15] and involves

1. Acidification of 350 ml polymer solution to pH 2 (using a Metrohm 716 DMS Titrino setup).
2. Dropwise addition of iron (III) chloride (0.2 M) to the stirred solution.
3. Neutralization to the desired pH (using a Metrohm 716 DMS Titrino setup). For higher molar iron: sulfate group ratios than 1:1, steps 1–3 have to be repeated up to a ratio of 2:1. For higher iron contents, another repetition is necessary and so on.

The procedure was modified as follows to produce magnetite. Fe^{2+} salt solution (freshly prepared in deoxygenated water) was added under a nitrogen atmosphere in the correct ratio (1:2) to the Fe^{3+}-loaded polymer solution at pH 2 (which was also previously flushed with nitrogen for at least 30 min). Potassium hydroxide (1 M) was used to raise the pH to above 10 as per Schwertmann and Cornell [26] and the system was flushed with nitrogen for a further 30 min. The characterization of the polymers used is summarized in Table 1.

The product formed by mineralization was characterized by X-ray diffraction (XRD), transmission electron microscopy (TEM), DLS, AUC, ultraviolet–visible absorption spectroscopy (UV–vis), and κ-carrageenan based species were further characterized by their electrophoretic mobility and optical rotation.

XRD (wide-angle X-ray scattering, WAXS, and small-angle X-ray scattering, SAXS) was performed on a PDS 120 (Nonius GmbH, Solingen) using Cu–K_α radiation ($\lambda = 1.54$ Å). WAXS refers to the conventional XRD diffractograms at 2θ angles greater than 10°, while SAXS diffractograms are obtained at angles less than 10°. TEM measurements were performed with a Zeiss EM912 OMEGA (Carl Zeiss, Jena) by diluting the samples in water and then drying straight onto a carbon-coated copper grid. The images obtained were analyzed using the AnalySIS software from SIS to obtain rough size estimates. Optical rotation was measured on a Perkin-Elmer 241, the accuracy being $\pm 0.002°$. A 10-cm cuvette was filled with the sample and the optical rotation was measured at room temperature (23 °C). The wavelength used was 589 nm (D line of sodium).

The DLS experiments used a laboratory-built goniometer with temperature control ($+/-0.05$ K), an attached single-photon detector ALV/SO-SIPD (ALV, Langen) and a multiple tau digital correlator ALV5000/FAST (ALV, Langen). The light source was

Table 1 Characteristics of the polymers used in this study

	Carrageenan κ	Carrageenan λ	Carrageenan ι	Cellulose sulfate
M_w (g/mol)	380 000[a]	330 000[a]	330 000[a]	97 000[b]
Sulfate content (mmol/g dry solids)[c]	2.7	4.1	3.3	2.6
Moisture content (%)[d]	10.2	8.37	8.83	7.6
Partial specific volume (g ml^{-1})[e]	0.4904	0.4552	0.4409	not measured

[a] Determined by sedimentation equilibrium analytical ultracentrifugation
[b] Determined by static light scattering
[c] Determined by titration with toluidine blue O and UV–vis spectroscopy [27]
[d] Determined by heating at 140 °C using an automated HR73 halogen moisture analyzer from Mettler Toledo to constant weight
[e] Determined in a DMA 60 (Anton Paar, Graz, Austria) density oscillation tube

an Innova 300 (Coherent, Santa Clara, USA) argon ion laser (488.0 nm, single-frequency mode, powered at approximately 800 mW). Several time-correlation functions were accumulated over a period of 5 min each. Only those whose baseline was not spoiled by particle-number fluctuations were subsequently inverse-Laplace transformed by using one of the many available regularization routines [28]. The resulting intensity-weighted apparent diffusion constant distributions were converted into the corresponding distributions of apparent hydrodynamic radii by employing the Stokes–Einstein equation. All samples were investigated by DLS at 90° scattering angle. DLS on the acidified κ-carrageenan (pH 2, 0.1 g l^{-1}) involved addition of iron (III) solution with an Eppendorf pipette and centrifugation at 7500 rpm for 5 min to remove dust particles. DLS on the other samples was performed at 2.0 g l^{-1} without centrifugation to avoid loss of the larger microgel particles.

AUC was performed on a Beckman Optima XL-I (Beckman Instruments, Palo Alto, Calif.) with integrated UV–vis absorption and on-line interference optics at 25 °C in a self-made titanium or commercial Epon double-sector centerpiece (depending on pH and the required run conditions). With the UV-absorption optics, only the iron-containing components could be selectively detected, whereas the simultaneous application of the Rayleigh interference optics yields the sedimentation profile of all components including the free polysaccharides which are transparent in the applied spectral range. The sedimentation coefficients were determined via the movement of the sedimenting boundaries, whereas the concentrations of the components were read from the differences between the upper and lower plateau values in the sedimentation profile. Fringe shifts were converted to concentration changes as described in Ref. [29]. All sedimentation coefficients given in this paper refer to 25 °C and are not extrapolated to infinite dilution. An example of an AUC run and its analysis is given in Fig. 2.

UV–vis spectra were obtained on a UVICON 931 (Kontron Instruments) spectrophotometer using 1-cm quartz cuvettes with distilled water as the reference. The hematite pigments were fractionated in gravitational and centrifugal fields and only the solids remaining in suspension after centrifugation at 10 000 rpm (9200 g) were used for the determination of the extinction coefficient. The solids were sonicated for 5 min prior to the measurement to ensure they were dispersed. The masses of the pigments in solution were determined from the solution density in a DMA 60 (Anton Paar, Graz, Austria) density oscillation tube. The average particle size was found to be 64 and 94 nm (by DLS) for Bayferrox 130M and 130, respectively.

Electrophoretic mobility was measured at pH 7 using a Malvern ZetaMaster ZEM5002 (Malvern Instruments, Southborough, USA) using the laser Doppler effect. The samples were equilibrated at 25 °C before the mobility was recorded in triplicate. The iron oxyhydroxide control (without polymer) was precipitated at pH 7 and was equilibrated overnight before the mobility measurement was conducted. The ionic strength was matched to the case when polymer is present because acid is added to the polymer solution. Iron oxyhydroxide solids aggregate at pH 7 so a peristaltic pump was used to equilibrate the slurry and to keep it suspended. The measurement was quickly taken after the pump was turned off. Particle sedimentation under these conditions was not appreciable.

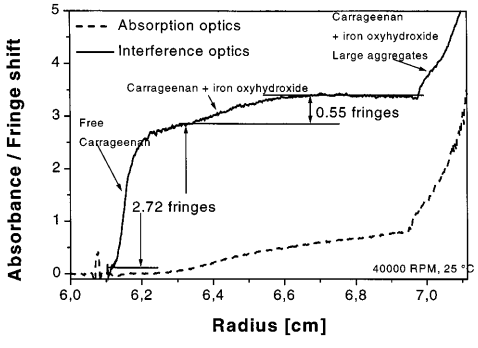

Fig. 2 Typical analytical ultracentrifugation experimental run showing the absorption and Rayleigh interference optics measurements

Materials

κ-Carrageenan (Copenhagen Pectin GENUGEL carrageenan type X-8944), ι-carrageenan (Copenhagen Pectin GENUVISCO carrageenan type X-8941) and λ-carrageenan (Copenhagen Pectin GENUVISCO carrageenan type X-8940) were obtained from Hercules. Cellulose-SO_4 (M_w = 97 000 g mol^{-1}, D_s = 0.5) was a kind gift from Horst Dautzenberg, University of Potsdam. Dextran sulfate from Aldrich was AR grade and had a nominal molecular weight of 5000 g mol^{-1}. Sodium hydroxide, hydrochloric acid and potassium hydroxide (all AR reagents obtained from Fluka Chemika and Aldrich) were used to control the pH for the various iron oxyhydroxide preparation methods. Iron (III) chloride hexahydrate and iron (II) chloride tetrahydrate (AR grade, Aldrich) were used as iron sources. As reference pigments for the comparison of exctinction coefficients, hematite samples Bayferrox 130M and 130 were obtained from Bayer, Uerdingen, Germany.

Results

The addition of $FeCl_3$ to a solution of acidified κ-carrageenan (or cellulose-SO_4 at molar iron/sulfate group ratios of up to 1:1 and the subsequent neutralization to pH 7–13 by sodium hydroxide does not result in any macroscopic precipitation. This is a strong indication that the polymer interacts with the iron oxyhydroxide. Within the pH range 3–13 transparent yellow to golden-brown solutions are obtained. Transparency of the colloidal solution was observed up to molar loadings of 100% Fe ions per polymer-bound SO_4 group (in the following denoted as Fe/SO_4). Higher loadings (greater than 100% Fe/SO_4) produced increasingly turbid solutions until a precipitate was observed at about 200%. Stability of iron oxyhydroxide colloids at such a high pH was not expected as previous work using dextran sulfate has only shown stability up to pH 11 [15]. The low-molar-mass dextran sulfate used in this work even showed no stabilization at all. Interestingly, ι-carrageenan only partially stabilizes at lower iron addition (about 80% Fe/SO_4), whereas λ-carrageenan showed a turbid solution even at 67% Fe/SO_4. This result demonstrates that significant stabilization of iron oxyhydroxide is only achieved with the applied polysaccharides carrying one sulfate group per repeat unit (two sugar rings). Hence only κ-carrageenan and cellulose-SO_4 were further investigated in this study.

While the results for κ-carrageenan and cellulose-SO_4 support those found in Ref. [15] the lack of stability with dextran sulfate does not; however, the dextran sulfate used in Ref. [15] had $M_w \approx 500\,000$ g mol^{-1}, which is a factor of 100 higher than that of the dextran sulfate used

in this study. Thus, the molecular weight seems to be relevant for stabilization. For the various carrageenans, gelling behavior and the associated change in size and structure also appear important.

Higher loadings of iron (resulting in transparent solutions) for both polysaccharides at a final pH of 7 could be achieved by repeating the acidification (to pH 2)/iron addition/neutralization steps (to pH 7). A total of 200% Fe/SO_4 was stabilized for κ-carrageenan and up to 300% Fe/SO_4 was stabilized for cellulose-SO_4.

Formation of magnetite at room temperature with mixed iron solutions is known to result in partial oxidation when the sample is in contact with air [26]. In the presence of the polymers, any magnetite formed (at 50–200% Fe/SO_4) turned from an initial black color to dark brown, indicating at least partial oxidation to maghemite in this case also.

X-ray diffraction

XRD on the dry powder polysaccharides showed no peaks for the polymers (data not shown).

The XRD data of the iron oxyhydroxide and carrageenan (Fig. 3, plot D) show no sharp reflections and only broad, weak XRD peaks at 2θ angles of 27° and 35°. The diffractogram is similar to that found by Coe and coworkers [18, 19] for iron oxyhydroxide–polysaccharide and iron oxyhydroxide–dextran complexes; however, the present peaks are broader. The iron oxyhydroxide phase produced is most likely a "cell-contracted akaganeite" (FeOOH) structure as referred to by Coe and coworkers [18, 19] or a two-line ferrihydrite but an unambiguous characterization is not possible because of the poor data quality. For iron oxyhydroxide and cellulose-SO_4 the diffractogram (Fig. 3, plot C) resembles that of the κ-carrageenan sample though the peaks are slightly more intense.

Magnetite formation in the presence of the polymers results in broad XRD peaks some of which match the peaks of pure magnetite. Other less well defined peaks are observable but could not be assigned to any particular phase. Magnetization curves indicated that superparamagnetic particles were formed in the presence of both polysaccharides.

Taking the reflection at $2\theta \sim 35°$, the crystallite size was calculated from the linewidth (Table 2). Independent SAXS analysis on the mineralized κ-carrageenan samples, which gives a weight-average particle radius, is also included. It is obvious that the crystallite size from WAXS is smaller than that obtained by SAXS, which can be attributed to disorder in the solid – especially iron oxyhydroxide; therefore, the crystallite sizes from WAXS can only be considered as estimates here.

Transmission electron microscopy

TEM of the sample with $FeCl_3$ added to κ-carrageenan at pH 2 clearly shows the gelling of the polymer to mesoscopic gel strings with a diameter of 10–50 nm (Fig. 4a). This is consistent with the macroscopically observed viscous/gelling solution behavior. With increasing pH the gel remains and nanoparticles inside more-or-less spherical microgels are observable (Fig. 4b). The individual nanoparticle size from TEM is of the same order of magnitude as revealed by SAXS.

The iron oxyhydroxide particles (pH 7) formed with cellulose-SO_4 present are shown in Fig. 5. The iron

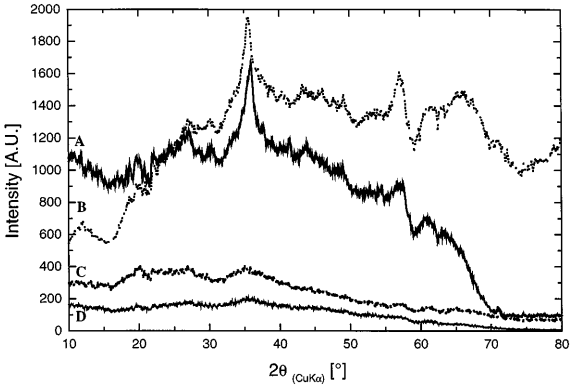

Fig. 3 X-ray diffraction (wide-angle X-ray scattering) of magnetite formation in cellulose-SO_4 at a Fe/SO_4 loading of 100% and pH 12 before ultrafiltration (*A*), magnetite formation in κ-carrageenan at an Fe/SO_4 loading of 100% and pH 12 before ultrafiltration (*B*), iron oxyhydroxide formation in cellulose-SO_4 at an Fe/SO_4 loading of 100% and pH 7 before ultrafiltration (*C*) and iron oxyhydroxide formation in κ-carrageenan at an Fe/SO_4 loading of 100% and pH 7 before ultrafiltration (*D*)

Table 2 Mean crystallite size as determined from X-ray diffraction and the weight-average particle radius as determined from small-angle X-ray scattering. All samples were at a molar ratio of 1:1 Fe^{3+} to sulfate. The iron oxyhydroxide samples were at pH 7 and the magnetite samples were at pH 12 before ultrafiltration

	Crystallite radius (nm)	Particle radius (nm)
κ-Carrageenan + iron oxyhydroxide (curve D)	1.0	7.8
Cellulose-SO_4 + iron oxyhydroxide (curve C)	1.6	Not measured
κ-Carrageenan + Fe_3O_4 (curve B)	5.5	6.6
Cellulose-SO_4 + Fe_3O_4 (curve A)	4.7	Not measured

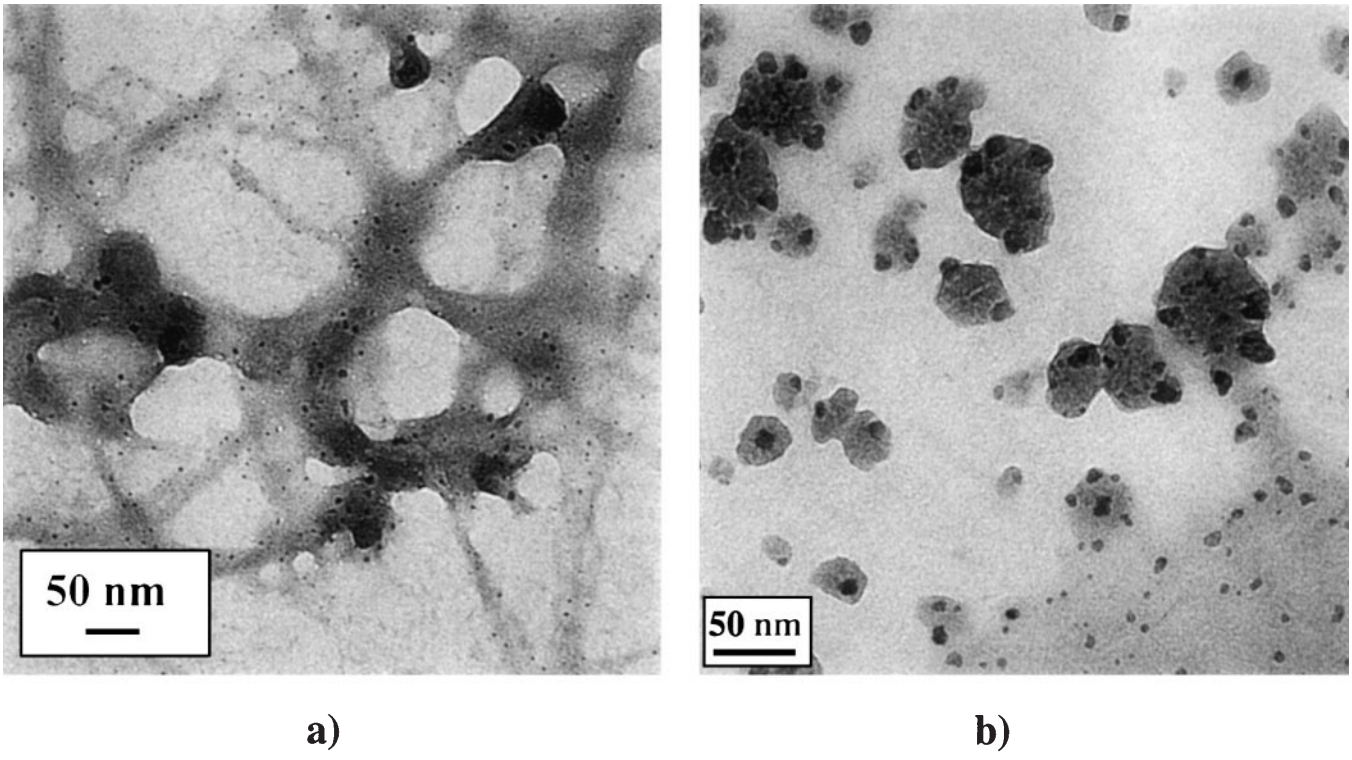

Fig. 4 Transmission electron microscope (TEM) image of Gel and nanoparticle formation of iron-loaded κ-carrageenan at **a** pH 2 and **b** pH 13. In both cases the iron loading was 100%

oxyhydroxide nanoparticles are polydisperse and have a diameter of about 10 nm. The particles are seen to aggregate on the grid, implying rather weak stabilization or a thin polymer layer. The structure depicted is presumably not the original structure but shows a tendency towards aggregation due to drying during the preparation of the TEM grid. For both κ-carrageenan and cellulose-SO_4 the sizes of the particles formed after $FeCl_3$ addition are similar to those (4–6 nm) previously found by Coe and coworkers [18, 19].

TEM pictures of the magnetite κ-carrageenan system showed particles very much aggregated within the gel (Fig. 6a). The particle diameters were about 20 nm, with the darker aggregates being of the order of 50 nm. TEM of the cellulose-SO_4 after magnetite formation showed almost completely separated nanoparticles which were in the 10–20-nm size range (Fig. 6b).

UV-vis

Both cellulose-SO_4 and κ-carrageenan are transparent at wavelengths longer than 210 nm, typical of polysaccharides. The $FeCl_3$–polymer system showed the expected absorption bands for Fe^{3+} solutions at pH 2 (242 and 345 nm) and at pH 3–11, where a broad absorption was detected [30].

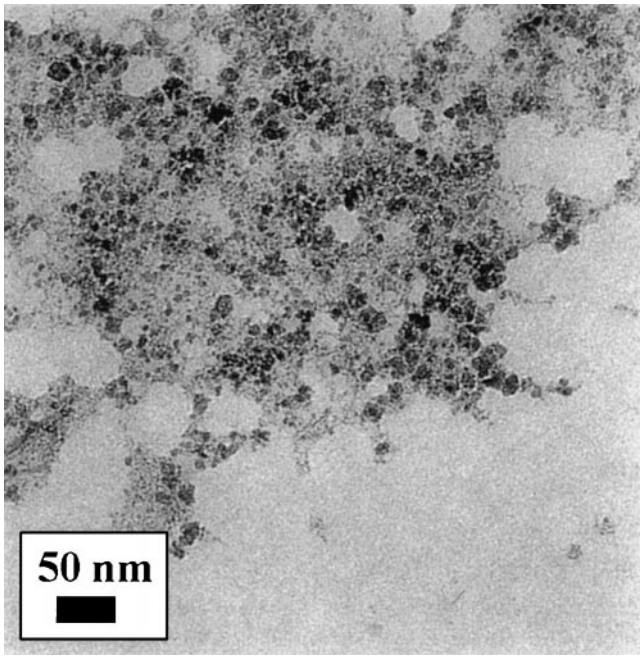

Fig. 5 TEM image of mineralized cellulose-SO_4 at an iron loading of 100% and pH 7

In order for an iron compound to be useful as a pigment high extinction coefficients are necessary (as a comparison, organic dyes have ε of the order of 10 000 $mol^{-1}\,l\,cm^{-1}$ and higher). To elucidate this

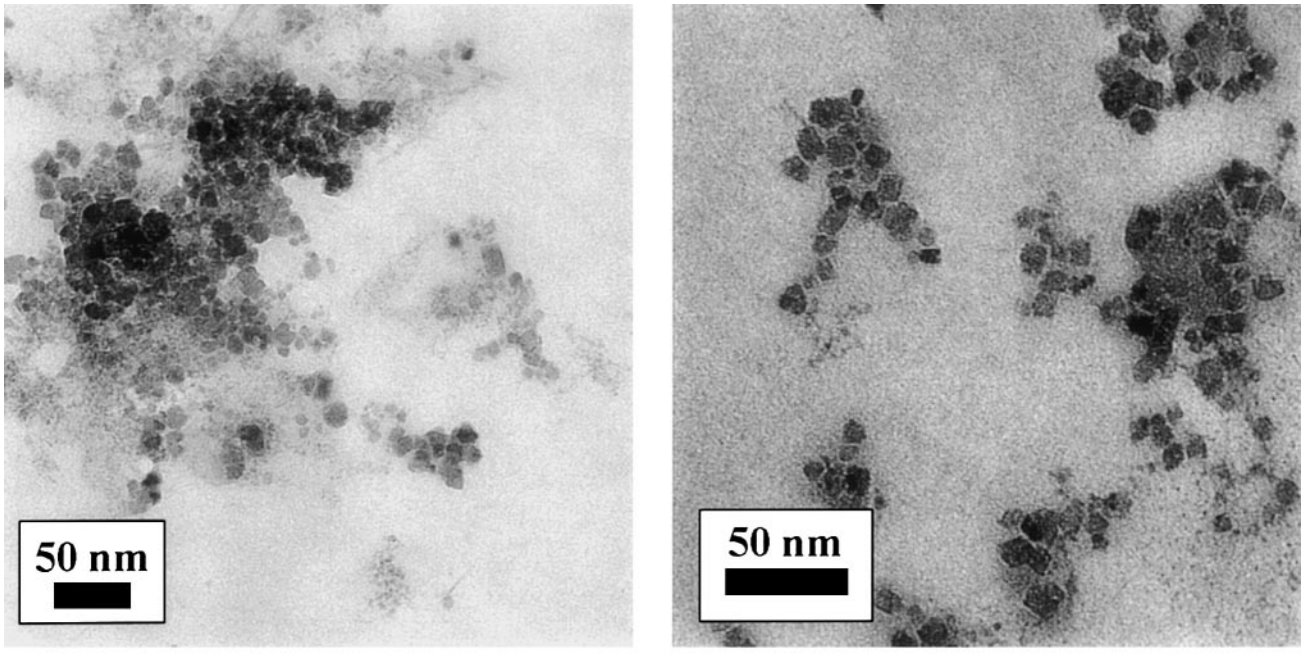

Fig. 6 TEM pictures of magnetite formation in **a** κ-carrageenan and **b** cellulose-SO_4. Both samples were at pH 12 and an Fe/SO_4 loading of 100%

application for the iron–polysaccharide systems, two commercial pigments (hematites) are compared to the iron-loaded κ-carrageenan with an Fe/SO_4 ratio of 100%, at pH 7 (Fig. 7). The cellulose-SO_4–iron oxyhydroxide hybrid has a similar absorption spectrum but with a higher maximum extinction coefficient of about 4900 $mol^{-1}\,l\,cm^{-1}$ (mol Fe^{3+}). The commercial pigments absorb over the whole visible spectrum, while the iron-loaded polymers have a very low extinction coefficient at wavelengths longer than 450 nm; however, at wavelengths below 300 nm the extinction coefficient is higher for the iron–carrageenan system. This means that these iron oxyhydroxide hybrids are very efficient blue- and UV-absorbing pigments.

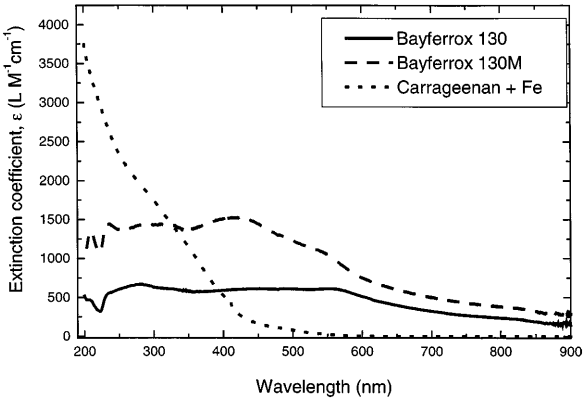

Fig. 7 Extinction coefficient of two hematite pigments (Bayferrox 130 and 130M, pH 7 in H_2O) and the mineralized iron in κ-carrageenan (pH 7, 100% Fe loading)

DLS and AUC

DLS measurements were used to judge if the particle/aggregate sizes found by TEM also exist in solution, i.e. are not due to concentration and drying on the TEM grid. The κ-carrageenan in water was found to have an average hydrodynamic radius of 45 nm, typical for this polymer of biological origin [32]. Addition of 60% Fe/SO_4 at pH 2 resulted in an immediate increase in the hydrodynamic radius to 150 nm, followed by a secondary growth (16 h or less) which produces a significantly wider size distribution and an average radius of approximately 700 nm. At pH 7 the DLS results show a bimodal distribution (Fig. 8). There is a fast-diffusing species which may be caused by the polyelectrolyte effect, unbound polymer fragments or nanoparticles which are not coupled to a larger polymer entity. The larger size fraction centre at 200 nm presumably represents the microgel or aggregated particles.

At pH 13 two peaks corresponding to sizes of 6 and 66 nm are observed, although the 6 nm peak is almost inperceptible; however, this would be in agreement with the previous observations in Fig. 4b, where 6 nm

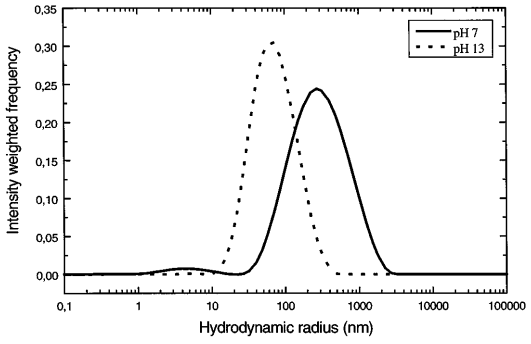

Fig. 8 Hydrodynamic size distribution (from dynamic light scattering) for iron oxyhydroxide mineralized κ-carrageenan at an iron-to-sulfate molar ratio of 100% and at pH 7 and 13

represents the individual nanoparticles and 66 nm is likely to be due to the aggregates/microgel. As the microgel diameter from TEM in Fig. 4b is approximately only 20 nm, the radius from DLS indicates a high volume swelling degree of 35.

DLS on the cellulose-SO_4 polymer without iron showed a bimodal distribution having average hydrodynamic radii of 67 and 906 nm, where the larger size can be attributed to the polymer behaving in a typical polyelectrolyte slow mode [33]. On addition of $FeCl_3$, a bimodal distribution is once again observed, and average hydrodynamic radii of about 90 nm and about 10 nm are calculated. As the salt addition leads to a breakdown of the slow mode, the 90-nm species is most likely the iron oxyhydroxide polymer hybrid, whereas the 10-nm species could correspond to the inorganic nanoparticles only loosely attached to the polymer. DLS results for magnetite formed in κ-carrageenan show an average radius of 527 nm (and an additional very weak fast-diffusing species). The much larger size in this instance compared to those of the iron oxyhydroxide–polymer hybrids (Fig. 8, pH 13, about 60 nm) possibly represents greater aggregation of the microgel. The K^+ ions used in the formation of magnetite are known to promote gelation of κ-carrageenan [22]. Magnetite in the nongelling cellulose-SO_4 on the other hand consisted of only one species with an average particle radius of 33 nm. TEM showed 10–20-nm particles; thus, it is seen that in solution the additional swollen polymer layer significantly contributes to the particle hydrodynamics. The hybrid particles are rather well defined in the solution state, indicating good colloidal stabilization.

As stated previously, AUC is able to discriminate between unbound and bound polymer and is thus able to give information on the different species present within the sample even in case of multicomponent systems. The presence of ''free'' iron oxyhydroxide particles could be excluded due to the number of interference fringes present. This is based on a calculation of the expected fringes for the case when the total iron in solution is present as unbound iron oxyhydroxide. The cross-linking of κ-carrageenan with the iron cations at pH 2 was further confirmed by AUC measurements. AUC of κ-carrageenan alone in aqueous solution (1.43 g l^{-1}) shows a sedimentation coefficient of 1.65 S (Table 3). At pH 2, the carrageenan with $FeCl_3$ added consisted of one species – carrageenan cross-linked with iron cations. As this was neutralized, two species could be differentiated which have been labeled ''free'' and ''bound'' carrageenan due to the magnitude of the sedimentation coefficients. The same is valid for cellulose-SO_4. The concentration of ''free'' carrageenan and of free cellulose-SO_4 drop with increasing iron content (Fig. 9) and remain constant at higher iron loadings. The limiting concentration of the free polymer of about 0.5 g/l is surprisingly high and is about 25% of the total polymer concentration.

Table 3 Sedimentation coefficient versus iron-to-sulfate molar ratio at pH 7. Results from analytical ultracentrifugation

Sedimentation coefficient	Iron-to-sulfate loading				
	0%	10%	30%	50%	100%
''Free'' carrageenan	1.65	1.65	1.58	1.98	2.11
''Bound'' carrageenan	–	5.50	5.30	17.17	22.92

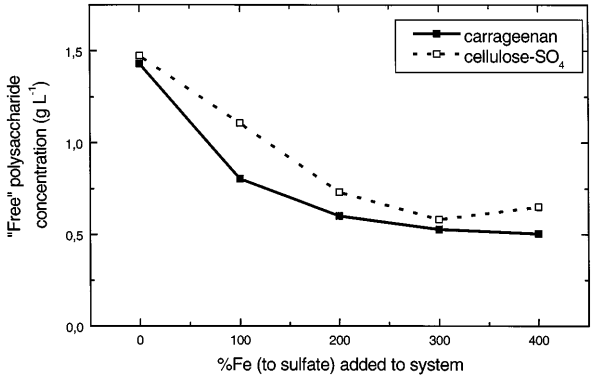

Fig. 9 ''Free'' polymer as determined from the Rayleigh interference optics of the ultracentrifuge for mineralized samples at pH 7

The ''free'' carrageenan sedimentation coefficient is similar to that of pure κ-carrageenan and increases slightly, whereas the ''bound'' carrageenan sedimentation coefficient increases significantly compared to that of the ''free'' κ-carrageenan (Table 3). It is remarkable that a sudden increase in the sedimentation coefficient between 30 and 50% iron loading is observed. For cellulose-SO_4 the change in the sedimentation coefficient with iron loading at a constant pH of 7 was found to be smaller than that for κ-carrageenan presented in Table 3. Even at low loadings, for example, 20% Fe/SO_4, the sedimentation coefficient was already high

(about 20 S), suggesting that larger iron oxyhydroxide particles are produced, as already seen in the TEM and DLS measurements.

The increase in sedimentation coefficient for the "bound" κ-carrageenan (and also for the cellulose-SO_4) can be attributed either to a size increase and/or to a density increase compared to the pure carrageenan. To check whether the observed increase is only due to a density increase caused by coordination of the iron oxyhydroxide to κ-carrageenan, the expected particle radius based on the Svedberg equation can be calculated from the sedimentation coefficient [34]. The density of the κ-carrageenan–iron oxyhydroxide complex is obtained by assuming a linear increase from pure κ-carrageenan to pure two-line ferrihydrite with the weight fraction of iron (III). The parameters weight fraction of 0.1935 at 100% Fe/SO_4, density of 2.4121 g ml^{-1}, M_w of 380 000 g/mol and $s = 23$ S at 100% Fe/SO_4 resulted in a hybrid particle diameter of 87 nm, which is considerably smaller than the radius of 200 nm from DLS (Fig. 8), and is in good agreement with the diameter of 90 nm for pure κ-carrageenan as found by DLS. Therefore, a significant increase in the molar mass and thus in the size due to aggregation of κ-carrageenan can be concluded.

When the iron loading is maintained at a constant value (100%) and the pH is altered both mineralized polymers show a sharp increase in the sedimentation coefficient at pH > 12. The iron cation is already fully hydrolyzed at pH 4–5 [35] so this cannot be due to formation of oxyhydroxide nanoparticles; however, the microgel becomes smaller upon the pH increase (as seen in Fig. 8, the size reduction of the large peak). Thus, the increase in the sedimentation coefficient at high pH may be due to the microgel becoming more compact.

The stability of the iron oxyhydroxide and κ-carrageenan microgel was investigated by AUC. The sample was left, after ultracentrifuging, for 17 days in the cell to reequilibrate and was then remeasured. No change in the volume of this fraction was observed. Since AUC is a sensitive tool to monitor structural changes in gels/microgels [36, 37] this confirms that the cross-linking density of the gel/microgel and its degree of swelling under pressure (accessible from the volume of the gel phase) has not changed. Analysis was then made as to whether the change from "free" to microgelled κ-carrageenan was or was not a reversible reaction. The concentration of the "free" polymer from the iron-loaded solution (pH 7) at various dilutions was obtained but showed no increase in the "free" κ-carrageenan ratio. Thus, the aggregation of the κ-carrageenan and the formation of the microgel is irreversible. This was confirmed by independent sedimentation equilibrium experiments on the same system (data not shown), where the concentration dependence of the apparent weight-average molar mass for a dilution series showed no master curve. This is a diagnostic for irreversible aggregation [38]. Thus the iron oxyhydroxide κ-carrageenan hybrid particles should be stable for long periods even to dilution or high pH.

AUC for both polysaccharides always showed "free" polymer present, which reached a steady-state concentration at high loadings (Fig. 9). If the plateau value is taken as the lowest possible concentration of "free" polymer it is clear that at lower iron loadings (below 300%) there is still polymer available to react with the iron (III) solution. The similarity of the behavior of both cellulose-SO_4 and κ-carrageenan implies that the presence of "free" polymer is not due to gelation.

Optical rotation and electrophoretic mobility

A 10 g l^{-1} solution of κ-carrageenan in water shows an optical rotation of $+0.510°$, at 2 g l^{-1} this is reduced to $+0.102°$. After mineralization the carrageenan (2 g l^{-1}) still showed optical activity with a rotation of $+0.090°$. The small difference of 12% between the two samples may represent a reduction in the number of helical structures on mineralization but could also be due to secondary effects. Nevertheless, it is seen that the helices are essentially preserved after mineralization.

The electrophoretic mobility of the κ-carrageenan (2 g l^{-1}) at pH 7 was -3.4 ± 0.13 $\mu m\ s^{-1}\ V^{-1}\ cm^{-1}$. The mobility of the carrageenan–iron oxyhydroxide hybrids was -3.6 ± 0.1 $\mu m\ s^{-1}\ V^{-1}\ cm^{-1}$ at pH 7 and was remarkably similar to that of the κ-carrageenan. Iron oxyhydroxide without polymer at pH 7 had a mobility of 0.1 ± 0.1 $\mu m\ s^{-1}\ V^{-1}\ cm^{-1}$. As the mobility value is determined by the surface charge (which is zero at pH 7 for ferrihydrite) this is in aggreement with literature values [39, 40]. The mobility is similar to that of the carrageenan and no sediment is observed. Thus, this supports other results demonstrating that the iron oxyhydroxide is within the κ-carrageenan microgel and is electrostatically invisible from the outside.

Discussion

The proposed model of stabilization of iron oxyhydroxide (or magnetite) mineralized in κ-carrageenan is shown in Fig. 10.

The Fe (III) cation hydrolyzes successively with increasing pH and is at least partially hydrolyzed (and polymerized) even at pH 2 [35].

The partially hydrolyzed iron cation at pH 2 interacts with the sulfate groups on the polymer.

DLS and AUC clearly show that addition of $FeCl_3$ to acidified κ-carrageenan results in an interaction between the carrageenan and the partially hydrolyzed iron cations. This can be understood in terms of a charge

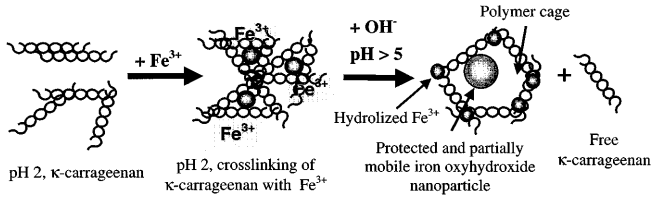

Fig. 10 Proposed model for nanoparticle stabilization in κ-carrageenan. For the sake of clarity, the figure is not drawn to scale

neutralization mechanism by which the sulfate groups on the κ-carrageenan are attracted by the addition of excess positive ions, which allows the carrageenan to aggregate [22]. At this pH only one species is observed by AUC. Thus, at this point the iron cations are homogeneously distributed throughout the solution. While the interaction between the iron (III) cation and the sulfate group is favorable on electrostatic grounds, the structure formed develops slowly. This slow aggregation may also indicate a low cross-linking strength between sulfate and iron.

At pH 2 no "free" carrageenan was observed (by AUC). The release of "free" carrageenan molecules into solution at pH 7 must therefore be a result of neutralization. It is assumed that the iron associated with a particular sulfate group has migrated to the growth centers of other nanoparticles, leaving unbound polymer behind. This is typical for a situation where the number of nucleation sites is below the number of microgel domains. This is observed in the uneven distribution of iron oxyhydroxide particles scattered throughout the microgel domains at pH 13 (Fig. 4b). Interaction of the polymer after neutralization with the nanoparticles results in a stable system.

The κ-carrageenan/iron oxyhydroxide hybrid system is shown to be stable for a long period of time (up to 10 months) even at pH 13. The only instability detected was due to microbial action rather than an intrinsic instability of the system. From the TEM picture in Fig. 4b, it is obvious that in case of κ-carrageenan the high stabiliziation is due to the formation of a cross-linked gel layer around the particle which protects the particle from contacting other particles and from aggregating to form a bulk precipitate. A comparison with the other carrageenans suggests that the induced gelation is advantageous to preserve stability. ι-carrageenan showed some stability, while λ-carrageenan – an only weakly gelling polysaccharide – did not.

Gel or microgel formation is not directly observed for the cellulose-SO_4 system. It is, however, known that cellulose sulfates are able to cross-link or form gels with K^+ ions or sufficient Ca^{2+} ions [41, 42]. Thus, a similar stabilization mechanism as proposed for the κ-carrageenan system in Fig. 10 may be discussed for cellulose-SO_4 due to the following observations.

1. Upon neutralization of the iron-loaded polymer system, a significant amount of polymer is released (more than 25% of the total concentration), leading to a distribution of iron-bound and free polymer.
2. The sedimentation coefficient increases significantly for the iron-bound polymer species.
3. DLS shows a bimodal distribution for both systems, most likely showing the aggregated polymer and the iron oxyhydroxide nanoparticles.

However, differences also exist. Figure 5 shows that there is no thick polymer layer around the inorganic particles as observed for κ-carrageenan (Fig. 4b). Furthermore, the sedimentation coefficient of κ-carrageenan increases jumpwise with increasing iron loading, whereas that of cellulose-SO_4 does not.

It may be assumed that as for the κ-carrageenan, cellulose-SO_4 is initially cross-linked with the iron cations then the remnant interactions with the iron oxyhyrdoxide surface after mineralization induce stability, releasing a certain part of the polymer as discussed for the κ-carrageenan system (Fig. 9). Clearly, due to the absence of the helical superstructure the "aggregation" of cellulose-SO_4 must be less than that of κ-carrageenan and this may play a role in its ability to stabilize higher iron loadings but also in the thickness of the stabilizing polymer shell.

The iron oxyhyrdoxide particles in cellulose-SO_4 are larger than in the κ-carrageenan case, possibly implying a higher mobility of Fe cations; however, the cellulose-SO_4 system showed less stability over time – some flakes were observed at pH 13 after 2 months. Thus, slow aggregation between particles due to reversible exchange of polymer is more facile in this system.

Magnetization curves indicated superparamagnetic particles when magnetite was formed in the presence of both polysaccharides. This is to be expected for maghemite particles smaller than 10 nm [31].

Conclusions and outlook

It has been demonstrated that iron oxyhydroxide nanoparticles are stabilized in solution in the presence of both cellulose-SO_4 and κ-carrageenan up to pH 13. The presence of iron cations in the polysaccharide solution induces cross-linking, which in turn creates a protective polysaccharide layer stabilizing a formed iron oxyhydroxide particle. The growth of the particles occurs in localized areas and results in free polymer being left in solution. Hence, at least the κ-carrageenan system can be considered as a self-assembled nanoreactor during iron addition and hydrolysis. Clearly, these polyelectrolytes are simple and environmentally friendly but are not ideal to both "bind" and "stabilize" the iron nanoparticles indefinitely. Block copolymers having a

sticking functionalized hydrophilic block and a stabilizing hydrophilic block (double hydrophilic block copolymers [43]) may be more appropriate in providing long-term stability.

AUC, DLS and TEM were used to characterize these hybrids. It was shown that the particles within the microgel are approximately 5 nm in radius, depending on pH and the phase produced. Mineralization in cellulose-SO_4 gives larger particles, of about 10 nm, stabilized with a thinner, noncrystalline polysaccharide layer. Such iron oxyhydroxide nanoparticles can be used for a wide variety of applications, including pigments, contrasting agents, nutrification or in dielectric and magnetic coatings. Niferex, for instance, is a commercial polysaccharide iron complex used to treat anemia [44]. Since most polysaccharide–iron complexes support the same iron oxyhydroxide phase [18, 19], the mineralized κ-carrageenan hybrid with its nontoxicity and its high pH stability may be an alternative for iron delivery.

Preparation of magnetite in the presence of the two polymers resulted in particle sizes of the order of 10 nm, but these particles cluster within the polymer matrix. In principle, all paramagnetic and ferromagnetic substances can be used to enhance the contrast in magnetic resonance images, and the nontoxic magnetite stabilized by a polysaccharide coating could be especially useful in all medical applications.

The small aggregates of iron oxyhydroxide nanoparticles are remarkably similar to those found in water sediments with natural organic matter as found by Buffle and coworkers [45–47], i.e. gel strings with nanoparticles of iron oxyhyrdoxides are seen. Thus, it may be that carrageenan is a good model for these systems and that these particles are stabilized by a similar protective coating mechanism.

Acknowledgements Many thanks go to H. Dautzenberg (University Potsdam) for the cellulose-SO_4 sample, R. Maibaum (University Duisburg) for the optical rotation measurements and discussion, T. Heinze (Friedrich Schiller University, Jena) for valuable discussion on cellulose-SO_4, I. Zenke for WAXS and SAXS measurements and H. Schnablegger for DLS measurements. Particular thanks go to B. Zilske and A. Völkel for the AUC work. M. Breulmann and W. Schwarzacher from the University of Bristol are acknowledged for the magnetization measurements. The Max Planck Society is acknowledged for financial support.

References

1. Schmid G (1994) Clusters and colloids: from theory to applications. VCH, Weinheim
2. Fendler JH (1996) Chem Mater 8:1616–1624
3. Pileni MP (1998) Cryst Res Technol 33:1155–1186
4. Meisel D (1997) Curr Opin Colloid Interface Sci 2:188–191
5. Herron N, Thorn DL (1998) Adv Mater 10:1173–1184
6. Mann S, Archibald DD, Didymus JM, Douglas T, Heywood BR, Meldrum FC, Reeves NJ (1993) Science 261:1286–1292
7. Addadi L, Weiner S (1992) Angew Chem Int Ed Engl 31:153–169
8. Weiner S, Addadi L (1997) J Mater Chem 7:689–702
9. Mann S, Webb J, Williams RJB (1989) Biomineralization. Chemical and biochemical perspectives. VCH, Weinheim, Germany, and references therein
10. Bauminger ER, Harrison PM, Hechel D, Nowik I, Treffry A (1991) Proc R Soc Lond Ser B 244:211–217
11. Wong KKW, Douglas T, Gider S, Awschalom DD, Mann S (1998) Chem Mater 10:279–285
12. Massover WH (1993) Micron 24:389–437
13. Bauminger ER, Harrison PM, Hechel D, Nowik I, Treffry A (1994) Hyperfine Interact 91:835–839
14. St Pierre TG, Chan P, Bauchspiess KR, Webb J, Betteridge S, Walton S, Dickson DPE (1996) Coord Chem Rev 151:125–143
15. Sipos P, St Pierre TG, Tombacz E, Webb J (1995) J Inorganic Biochem 58:129–138
16. Chan P, Chua-anusorn W, Nesterova M, Sipos P, St Pierre TG, Ward J, Webb J (1995) Aust J Chem 48:783–792
17. Bereman RD, Berg KA (1989) Inorg Chim Acta 155:183–189
18. Coe EM, Bowen LH, Speer JA, Wang Z, Sayers DE, Bereman RD (1995) J Inorg Biochem 58:269–278
19. Coe EM, Bereman RD, Monte WT (1995) J Inorg Biochem 60:149–153
20. Coe EM, Bowen LH, Speer JA, Bereman RD (1995) J Inorg Biochem 57:287–292
21. Coe EM, Bowen LH, Bereman RD, Speer JA, Monte WT, Scaggs I (1995) J Inorg Biochem 57:63–71
22. Therkelsen GH Chapter 7 in Whistler RL, BeMiller JN (1993) Industrial gums. Academic Press, London, 145–180
23. Piculell L, Borgström J, Chronakis IS, Quist P-Q, Viebke C (1997) Int J Biol Macromol 21:141–153
24. Michel A-S, Mestdagh MM, Axelos MAV (1997) Int J Biol Macromol 21:195–200
25. Morris ER, Rees DA, Robinson G (1980) J Mol Biol 138:349–362
26. Schwertmann U, Cornell RM (1991) Iron oxides in the laboratory. Preparation and characterization. VCH, Weinheim
27. Wassmer KH, Schroeder U, Horn D (1991) Makromol Chem 192:553–565
28. Schnablegger H, Glatter O (1991) Appl Opt 30:4889–4896
29. Schachman HK (1959) Ultracentrifugation in biochemistry. Academic Press, New York, p43
30. Mulay LN, Selwood PW (1955) J Am Chem Soc 77:2693–2701
31. Coey JM, Khalfalla D (1972) Phys Status Solidi A 1:229–241
32. Norton IT, Goodall DM, Morris ER, Rees DA (1983) J Chem Soc Faraday Trans I 79:2475–2488
33. Schmidt M, Förster S (1995) Adv Polym Sci 120:92–105
34. Svedberg T, Pedersen KO (1940) Die Ultrazentrifuge. Steinkopff, Dresden
35. Cotton FA, Wilkinson G (1980) Advanced inorganic chemistry. 4th edn. Wiley, New York
36. Cölfen H (1995) Colloid Polym Sci 273:1101–1137
37. Cölfen H (1999) Biotechnol Genet Eng Rev 87–140
38. McRorie DK, Voelker PS (1993) Self-associating systems in the analytical ultracentrifuge. Beckman Instruments, Fullerton, Calif.
39. Parida KM, Gorai B, Das NN, Rao SB (1997) J Colloid Interface Sci 185:355–362

40. Garcell L, Morales MP, Andres-Vergés M, Tartaj P, Serna CJ (1998) J Colloid Interface Sci 205:470–475
41. Fleury E, Dubois J, Léonard C, Joseleau JP, Chanzy H (1994) Cellulose 1:131–144
42. Philipp B, Wagenknecht W, Holzapfel G (1985) Cellul Chem Technol 19:331–339
43. Sedlak M, Antonietti M, Cölfen H (1998) Macromol Chem Phys 199:247–254
44. Piccinni L, Ricciotti M (1982) Panminerva Med 24:213–220
45. Buffle J, Leppard GG (1995) Environ Sci Technol 29:2169–2175
46. Pizaro J, Belzile N, Filella M, Leppard GG, Negre JC, Perret D, Buffle J (1995) Wat Res 29:617–632
47. Buffle J, Wilkinson KJ, Stoll S, Filella M, Zhang J (1998) Environ Sci Technol 32:2887–2899